Continental Shelf Research 124 (2016) 83–94

Contents lists available at ScienceDirect

Continental Shelf Research

journal homepage: www.elsevier.com/locate/csr

Research papers

Recent morphodynamic evolution of the largest uninhibited island in the Yangtze (Changjiang) estuary during 1998–2014: Influence of the anthropogenic interference

Wen Wei [a], Xuefei Mei [a], Zhijun Dai [a,*], Zhenghong Tang [b]

[a] State Key Lab of Estuarine & Coastal Research, East China Normal University, Shanghai 200062, China
[b] Community and Regional Planning Program, University of Nebraska-Lincoln, USA

ARTICLE INFO

Article history:
Received 4 December 2015
Received in revised form
20 May 2016
Accepted 23 May 2016
Available online 24 May 2016

Keywords:
Morphodynamic evolution
Sediment flux
Estuarine engineering
Jiuduan Shoal
Yangtze River (estuary)

ABSTRACT

Estuarine geomorphology worldwide has greatly changed in the Anthropocene due to intensive human inferences in river basin and within estuary, which has received increasing global concerns. Here, recent morphodynamic evolution of Jiuduan Shoal (JDS), the largest uninhabited island in the Yangtze (Changjiang) Estuary, and associated controlling factors were analyzed based on unique high-resolution seasonal-surveyed bathymetric data during 1998–2014. It can be indicated that JDS presents novel 12 and 48 months fluctuations though significant accretion was detected on high flats above −2 m. Meanwhile, morphodynamic evolution of JDS during 1998–2014 was divided into three stages: significant siltation on landward half of north JDS and expanding of Jiangya Shoal (JYS, part of JDS) tail, but less accretion at high flats from 1998 to 2002; continuous variations of JYS and reshape of seaward JDS with erosion band and heave appearance from 2002 to 2006; retentive alteration of JYS but recovery of erosion band and heave, together with redistribution of sand between high and low flats on seaward JDS after 2007. Moreover, river discharge could be likely the key factor controlling periodic characteristics of recent JDS evolution. Deep waterway project (DWP) dominates area increase of JDS by inducing accretion in north edge and south edge of Lower Shoal between 1998 and 2014.

1. Introduction

Distributary bar, protruding among estuarine geomorphology and manifesting as sink of sediment, is a highly dynamic structure, whose size, shape, even location change with variant sediment input and driving forces (Rubin et al., 1980; Ashley, 1990; Francken et al., 2004; Bartholdy et al., 2005). Besides, distributary bar commands diffluence of lateral channels, development of which significantly hinder maritime industry in bilateral branching channels. Thus, it is extremely essential to grasp morphodynamic evolution of distributary bar, not only for scientific purpose like sediment dynamics, but also for realistic meaning such as waterway maintenance. Considering its prominent role in purifying water, controlling floods, recycling nutrients and sustaining biodiversity, understanding status and evolution of distributary bar is also of remarkable ecological significance (Ramsar, 2007).

Distributary bar is vulnerable under anthropogenic disturbances due to its highly dynamic nature. On one hand, distal anthropogenic activities in drainage basin, including river damming, river diverting, irrigation, as well as land-use change, have decreased sediment delivering to estuaries all over the world, and triggered recession of estuarine sandbar in many rivers, like Nile River, Mississippi River and Yellow River (Milliman et al., 1987; Fanos, 1995; Syvitski et al., 2005; Xu, 2008; Blum et al., 2009). On the other hand, estuarine hydraulic engineering, such as dredging for waterway and reclamation projects, have altered estuarine dynamics and sedimentation process corresponding distributary bar (Benedet et al., 2008). Examples can be seen in estuaries worldwide: Dredging activities in channel of the Ribble estuary, northwest England concentrated the ebb flow in the over-deepened channel, enhancing sedimentation (Van der Wal et al., 2002); Reclamation leads to discharge loss and poor sedimentation on Sydney estuary (McLoughlin, 2000). The intercoupling of these artificial factors makes the evolution of distributary bar more complex.

Up to now, some studies have been carried out on natural morphodynamics in a variety of environments, covering river (Harbor, 1998; Carling et al., 2000; Harrisa et al., 2004), estuary (Kostaschuk, et al., 1989; Cuadrado et al., 2003; Jia et al., 2013;

* Corresponding author.
E-mail address: zjdai@sklec.ecnu.edu.cn (Z. Dai).

http://dx.doi.org/10.1016/j.csr.2016.05.011
0278-4343/

Raston et al., 2013; Wang et al., 2013; Nagarajana et al., 2015), coast (Chaumillon et al., 2008) and continental shelf (Flemming, 1978; Corbetta et al., 2006). Due to increasing influence of anthropogenic activities on estuarine morphology, researches on response of estuarine morphodynamic evolution to estuarine engineering are also conducted widely (Lafite et al., 2001; Kim et al., 2006; Bale et al., 2007; Jaffe et al., 2007; Syvitski et al., 2007; Lee and Ryu, 2008). However, little has been focused on morphodynamic evolution of distributary bars under influence of estuarine artificial engineering and catchment human interference.

Yangtze (Changjiang) River, the largest river in the Eurasian continent, flows through a distance of 6300 km, holds a population of over 4×10^8 and delivers plentiful fluvial materials to its terminal, the Yangtze estuary (Yang et al., 2011). Nearly half of the sediment is deposited in the river mouth region, forming a series of longitudinal sand bars, among which Chongming, Hengsha, Changxing and Jiuduan Shoal (JDS), sequentially bifurcate the river channel and constitute a configuration of 3 order bifurcation and 4 outlets into the East China Sea (Chen et al., 1999). JDS, the third generation of isolated island, plays a tremendous role in maintaining stability of the South and North Passage before 1990s It is also the largest uninhabited island in the Yangtze Estuary and full of ecological value as a national natural wetland reserve declared by the Chinese government in 2005 (Gao et al., 2010).

JDS has experienced dramatic morphodynamic changes to adjust to the new channel structures of Yangtze estuary since its birth (Xie et al., 2009). In recent two decades, intensive artificial engineering has been operated, which would affect JDS evolution significantly. Green engineering was conducted in JDS for ecological protection after 1990, which promotes accretion on high flats of JDS (Yun, 2010). Meanwhile, due to water and soil conservation policy and vast dam constructions, especially the world's largest dam, the Three Gorges Dam (TGD, operated in 2003), sediment delivered to estuary has decreased sharply, from 5×10^8 t/yr in the 1950 s to less than 1.5×10^8 t/yr after 2003 (Dai et al., 2014). Riverine load available to JDS decreases accordingly, which could have some effects on JDS evolution. Furtherly, the largest estuarine hydraulic engineering in China, Deep Waterway Project (DWP), is conducted at North Passage during 1998–2010 for shipping trade (Fig. 1b and c). The project proceeds in 3 phases and finally increases Yangtze Estuary's main shipping channel depth from less than 7 m to about 12.5 m. 2 dikes, 10 groins and a diversion work

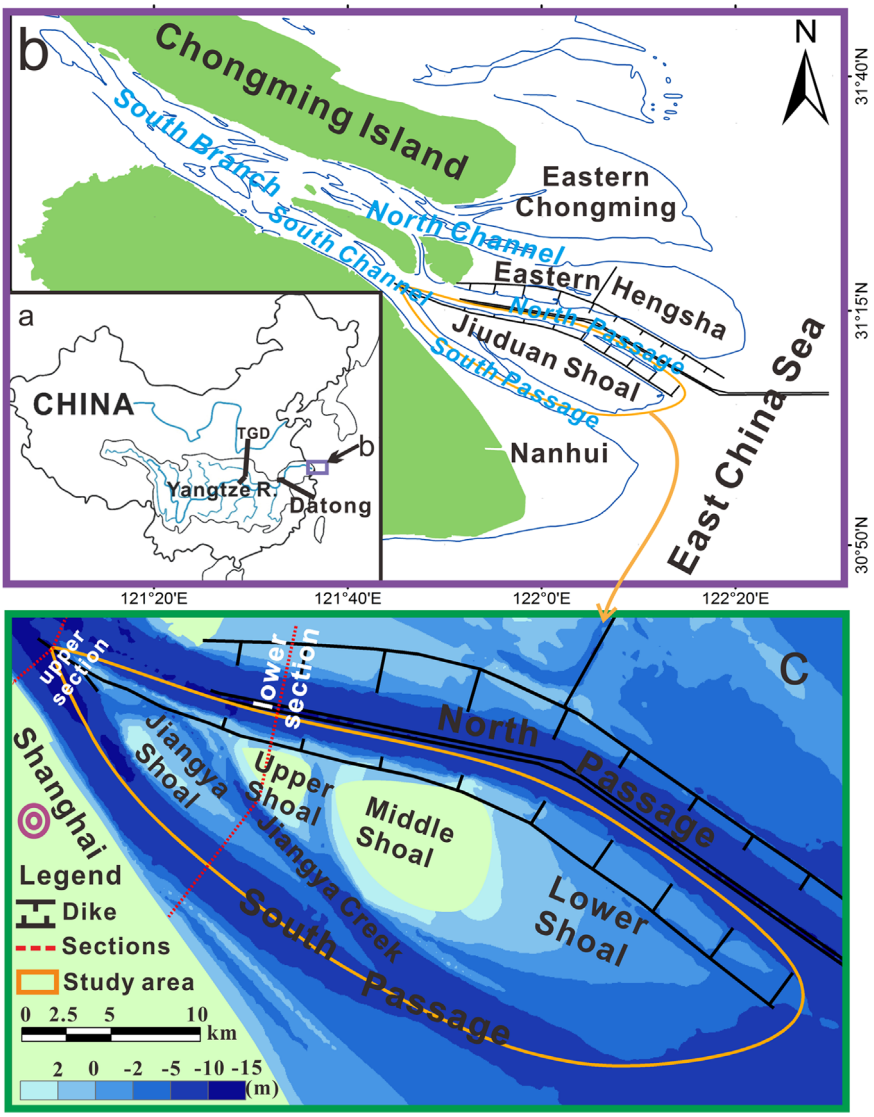

Fig. 1. Maps of (a) China showing the drainage basin of the Yangtze River, locations of TGD and Datong station; (b) geographic setting of the Yangtze estuary, JDS and surrounding channels, orange circle represents study area for bathymetric changes and eigenanalysis; and (c) diagram showing landform of JDS (surveyed in 08.2007) and configurations of sections for calculating ebb flow diversions ratio. (For interpretation of the references to color in this figure legend, the reader is referred to the web version of this article.)

at distributary inlet of North and South Passage were constructed with dredging rate of nearly 16 Mt/yr during 01.1998–05.2001, increasing the waterway's depth to 8.5 m. The two dikes were extended seaward, 5 groins constructed in former stage were prolonged and 9 new longer groins were constructed during 05.2002–03.2005. Depth of waterway reached 10 m with an annual dredging rate of more than 40 Mt/yr. No additional facilities were built but high rate of dredging (more than 60 Mt/yr) was carried out to deepen waterway depth to 12.5 m during 09.2006–03.2010. Considering its magnitude and proximity to JDS (with south dike constructed along JDS), DWP would also play some roles in JDS evolution.

Although some studies indicated that the JDS had seaward depositional trends due to impacts of natural factors between 1950 and 1990s, and vertical accretion over −2 m isobaths under the DWP impacts after 1998 (Xie et al., 2009; Gao et al., 2010), little attention has been given to recent evolution of JDS in response to anthropogenic activities from upstream and estuary itself. Due to limited data source, the previous researches on evolution JDS are based on the Landsat images or low re-resolution sea-maps (Jiang et al., 2012; Zheng et al., 2013), which fail to detect finely morphodynamic changes of JDS in response to different human disturbance.

Therefore, with the newly and unique survey bathymetric data during 1998–2014, the purposes of this paper are to: 1) explore recent morphodynamic evolution of JDS, 2) assess the relative importance of possible driven factors on JDS morphodynamic changes, and 3) discrimination the recent evolutionary stages of JDS.

2. Data and methods

Bathymetric data is of prime importance in quantitative research of morphodynamic evolution and sediment dynamics in estuaries (van der Wal and Pye, 2003; Blott et al., 2006). Here, data from 35 contiguous high-precision bathymetric surveys are collected from the Changjiang Estuary Waterway Administration Bureau (CJWAB), Ministry of Transportation (homepage: www.cjkhd.com) (Table 1). The surveys are undertaken seasonally on a semi-annual basis covering JDS and lateral passages (North Passage and South Passage), mostly in February and August based on the theoretical low-tide datum on scale of 1:25,000 (before 2004) and 1:10,000 (after 2004). Besides, dual-frequency echo sounders are used in depth measurement with a vertical error of 0.1 m and GPS devices by Trimble, USA are used for positioning with error within 1 m.

To explore impacts of riverine load on JDS evolution, monthly water discharge and suspended sediment flux data during 1998–2014 at Datong Station (the tidal limit of the Yangtze estuary), are acquired from the Bulletin of China River Sediment (BCRS) (available at: www.cjh.com.cn/). To further diagnose altered hydrodynamic environment of lateral passages under JDS evolution, data on ebb flow diversion ratios of the North Passage and the South Passage during 1997–2012 are also gained from CJWAB.

Raw bathymetric data are firstly transferred onto Beijing 54 coordinates and calibrated into 'Wusong Datum' in ArcGIS 10.1. Generally, there are dead zones in bathymetric data resulting from unavailability of surveys on top of JDS, which are variant in different surveys. Thus 2 blank areas are built (the two circles inside JDS in Fig. 1c) as common dead zones, inside which data points of each survey are removed to generate uniform dataset. Subsequently, data of each survey are gridded by Kriging interpolation method into 50 m to build digital elevation model (DEM). Area of JDS above given depths (0, −2 and −5 m) are calculated as the envelope area of corresponding isobaths, which are extracted from DEM. The calculated area of JDS above 0 m during 2.2000–2.2001 are significantly affected since dead zones of these years are beyond 0 m isobaths, while that in other years is slightly affected. Subsequent analysis on area changes of JDS above 0 m is continued, while that on 0 m isobaths is canceled.

In order to gain primary evolution mode of JDS and explore implications of each mode, Empirical Orthogonal Function (EOF) is applied, which serves as an efficient statistical technique functioning in many domains, such as meteorology, oceanography, geology, sedimentology and geomorphology (Yoo and Kim, 2004). With this method, the complex origin dataset can be decomposed into a linear combination of relatively small numbers of spatial and temporal patterns, named eigenvectors (spatial eigenfunctions) and eigenweighings (temporal eigenfunctions), separately (Dai et al., 2010). Generally, the first few eigenfunctions are sufficient to reflect main information of original dataset. Besides, each pair of spatial/temporal eigenfunctions represents a different independent mode of original dataset and can be analyzed separately due to the orthogonal property of eigenfunctions. Algorithm of EOF can be described in detail as follows (Dai et al., 2010):

Firstly, acquire the covariance matrix U of the original dataset (X), where $X=(X_1, X_2 \ldots X_N)$ with N surveys sorting in rows and make $U=XX'$.

Secondly, the eigenvalues λ ($\lambda_1, \lambda_2, \ldots \lambda_M$) and eigenvector

Table 1
Bathymetric surveys covering JDS, Yangtze Estuary, by CJWAB.

Year	February	May	August	September	November	December	Scale
1998				✓			1:25,000
1999	✓		✓				1:25,000
2000	✓		✓				1:25,000
2001	✓		✓				1:25,000
2002	✓		✓		✓	✓	1:25,000
2003	✓		✓				1:25,000
2004	✓		✓				1:10,000
2005	✓		✓				1:10,000
2006	✓		✓				1:10,000
2007	✓				✓		1:10,000
2008		✓			✓		1:10,000
2009		✓			✓		1:10,000
2010	✓		✓				1:10,000
2011	✓		✓				1:10,000
2012	✓		✓				1:10,000
2013	✓		✓		✓		1:10,000
2014			✓				1:10,000

Note: Topographic campaigns are marked with purple areas.

(V) of U can be obtained to satisfy the equation of $CV=V\lambda$. Thereafter, the eigenweighing (T) is calculated by $T=V'X$.

Thirdly, rearrange the eigenfunctions (both V and T) by the corresponding eigenvalues (λ) in order (from the largest to the smallest) and the variance contribution R_i of each eigenfunction can be calculated as $R_i = \lambda_i / \sum_{i=1}^{N} \lambda_i$.

Fourthly, ascertain the appropriate number of eigenfunctions to interpret the original dataset by making the cumulative contribution exceeding 85%.

In order to detect multiple-scale fluctuations in JDS evolution, continuous wavelet transform is applied to the area series of JDS (Torrence and Compo, 1998). The continuous wavelet transform of signal x(t) can be expressed by:

$$W(a, b) = < x(t), \varphi_{a,b}(t) > = \int_{-\infty}^{+\infty} x(t)\varphi^*_{a,b}(t)dt = \frac{1}{\sqrt{a}} \int_{-\infty}^{+\infty} x(t)\varphi^*\left(\frac{t-b}{a}\right)dt \quad a, b \in R, a \neq 0, \tag{1}$$

where a and t are scale and time parameters, $\varphi(t)$ and $\varphi^*(t)$ are wavelet basis functions and the complex conjugate of the wavelet coefficient, respectively.

The complex Morlet wavelet is selected as basis wavelet function:

$$\varphi(t) = \frac{1}{\sqrt{\pi f_b}} e^{i2\pi f_c t - (t^2/f_b)}, \tag{2}$$

where f_c is the central frequency of the mother wavelet, and f_b is the bandwidth.

Table 2
Area evolution of JDS in different stages.

Increasing[a] rate (km^2/yr)	Stage 1	Stage 2	Stage 3	Whole period
Above 0 m	1.53	5.04	3.46	4.57
Above −2 m	1.87	5.16	−1.01	2.42
Above −5 m	3.60	−0.27	2.07	2.19

[a] Area increasing rate is gained by linear fitting, as shown in Fig. 2.

3. Results

3.1. Area changes of JDS

Despite gradually increasing tendency, area changes of JDS varies in different depths (Fig. 2; Table 2). Between 1998 and 2014, area of JDS above 0 m presents the most significant increase with a rate of 4.57 km^2/yr. However, increasing rates of area above −2 m and −5 m are relatively slow, being 2.42 and 2.19 km^2/yr, respectively. Considering the small original value (117.41 km^2 in 1998.09) and the large increasing rate, flats above 0 m expand remarkably by 61.27% in the whole period. In brief, the higher, the faster it expands for JDS.

Specifically, area of JDS presents stage changes, which is divided according to DWP engineering phases (Fig. 2). Start and end time of each stage and corresponding area increasing rates are summarized in Table 2. In Stage 1, area over different isobaths increase continuously, among which area above −5 m indicates the fastest increasing rate of 3.60 km^2/yr. The subsequent Stage 2 is high-speed expanding period for area above 0 m and −2 m, during which their areas increase at rates of 5.04 and 5.16 km^2/yr. However, area above −5 m decreases slightly. During Stage 3, area above 0 m continues increasing with a slight lower increasing rate of 3.46 km^2/yr. Area above −2 m turns from high-speed increasing to decreasing at a rate of 1.01 km^2/yr while area above −5 m starts to increase at a rate of 2.07 km^2/yr. Variations in area changes above different depths in different stages reflect that higher and

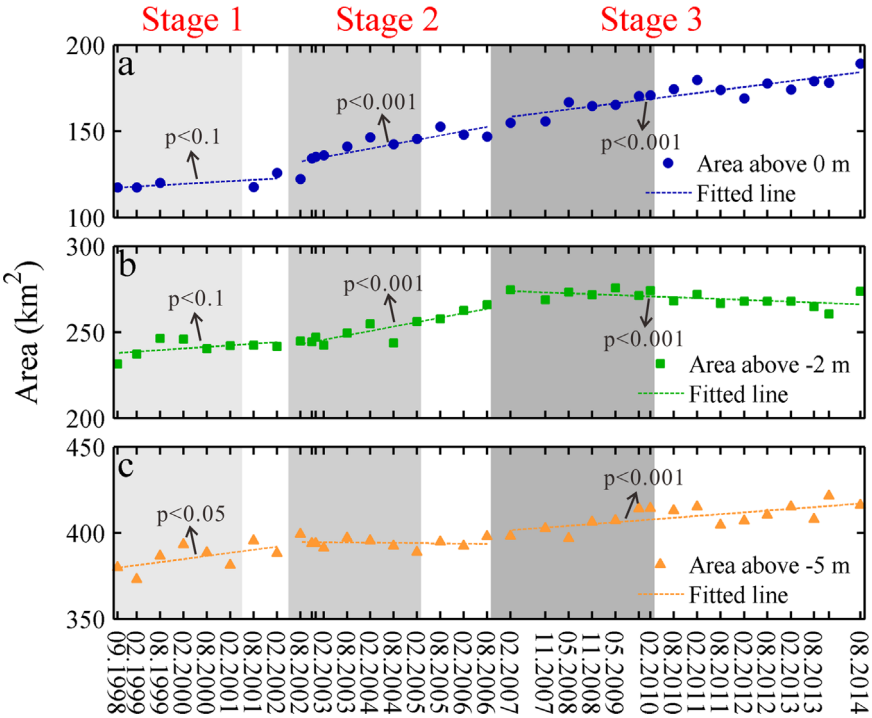

Fig. 2. Area changes of JDS (a) above 0 m; (b) above −2 m; and (c) above −5 m. 3 phases for DWP are depicted by the 3 grey area, with color gradually deepening. Trend lines for each stage are also shown by linear fitting.

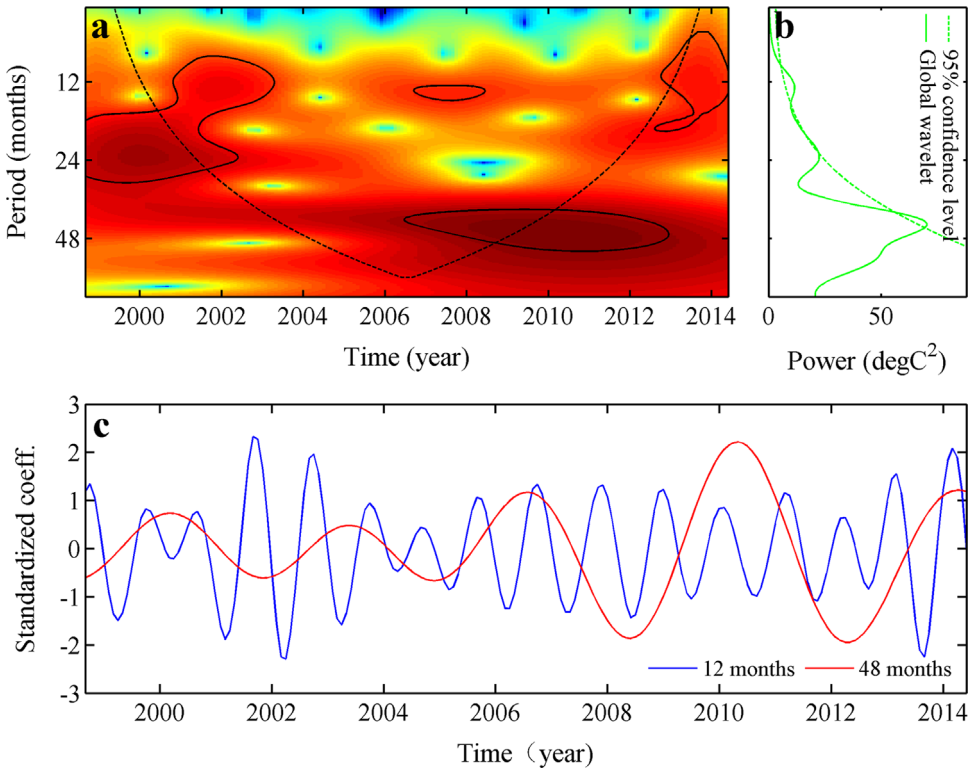

Fig. 3. Wavelet analysis on area changes of JDS above −5 m: (a) contoured coefficient; and (b) time series of periods (namely 1, 3–4 and 6–7 yr) extracted from corresponding contours.

lower flats of JDS have discrepancies in responding to DWP.

Meanwhile, it is obvious that relative significant fluctuations exist in area of JDS above −5 m, shown by scatters along trend line (Fig. 2c). Then detrend of above −5 m area series is processed by wavelet analysis to gain involved fluctuation components. Dramatic periods of 12 and 48 months can be detected, which indicates annual and quadrennial fluctuations in size evolution of JDS (Fig. 3a and b). However, no significant periodic fluctuations could be found for area above 0 m and −2 m. In fact, magnitude of 48 months fluctuation is an order larger than that of 12 months period, indicating dominant role of 48 months period in fluctuation components and standardized coefficient time series are depicted for better demonstration (Fig. 3c).

3.2. *Bathymetric changes of JDS*

With DWP proceeding, JDS leaves from its original shuttle shape with smooth boarder to become a little malformed, together with re-adjustment of internal components (Fig. 4). Furtherly, it can be seen from Figs. 4–6 on the representative morphological and bathymetric changes of JDS between and within each stage.

In Stage 1 (09.1998–02.2002), the most significant changes occur at landward half of JDS. Project region of the first engineering phase, which locates in landward half of north JDS, develops wavy morphology due to dramatic siltation. Landward half of JDS expands northward, especially in 02.2001, and Jiangya shoal-creek system undergoes great changes (Figs. 4a, b and 5b). Tail of Jiangya Shoal (JYS) stretches dramatically into the South Passage in 02.2000 and 02.2001, with direction rotating gradually anticlockwise. Head of JYS extends landward with an isolated sandbar formed during 2000. Jiangya Creek, which used to serve as flood channel for the South Passage, migrates eastward by eroding the Upper and Middle Shoal and retreats southeastern gradually. Besides, −2 m isobaths of Jiangya Creek extends upward along the south dike and connects with the South Passage at the entrance in 08.2001 (Fig. 5a). Creek between Upper Shoal and Middle Shoal disappears after 02.2002. Meanwhile, deposition on high flat of south Lower Shoal made −2 m isobaths there more symmetric since 02.1999 (Figs. 4a, b and 5a). Though those zones experience extensive siltation or erosion, the cumulative deposition volume for Stage 1 is nearly zero (Fig. 6a and d). Thus during Stage 1, JDS and surrounding channels gain no net sediment, but experience sediment redistribution between flats and channels within the study area.

In Stage 2 (08.2002–08.2006), significant changes appear at seaward half of JDS due to the extended south dike in the second engineering phase, which makes this stage unique. In 2005, high flats just south of the south dike on Lower Shoal suffer erosion, forming an erosion band there shown by the incurvate −2 m isobaths around dike (Figs. 4d and 5c). Significant siltation occurs on flats north of dike with wavy morphology spreading downstream signally around 08.2004. −5 m isobaths expands along dike deeply into the sea, holding the last groin and forming a heave. Southern Lower Shoal experiences erosion with shape of −2 m isobaths on Lower Shoal changing a little and a small sandbar is leaving away from southern Middle shoal with their −2 m isobaths separated. Former evolution of Jiangya Shoal-creek system continues, despite the gradually upward extending −5 m isobaths of Jiangya creek, and tail of JYS stretches to shipping lane of the South Passage in this stage (Figs. 4c, d and 5d). Siltation of Stage 2 concentrates on area north of dike, eastern JYS and flats above 0 m on Lower Shoal, while erosion exists sporadically and is usually not severe, making this stage the most dramatic siltation stage at a rate of 0.028 km^3/yr (Fig. 6b and d).

In Stage 3 (02.2007–08.2014), since no additional artificial facilities are constructed and only dredging activities continue, bathymetric changes of JDS are not so significant as the former 2 stages (Fig. 6c). Annual deposition of this stage is relative large (0.019 km^3/yr) due to continuous accretion of high flats, which is obvious in DEM (Figs. 4e, f and 6d). Bathymetric changes of south

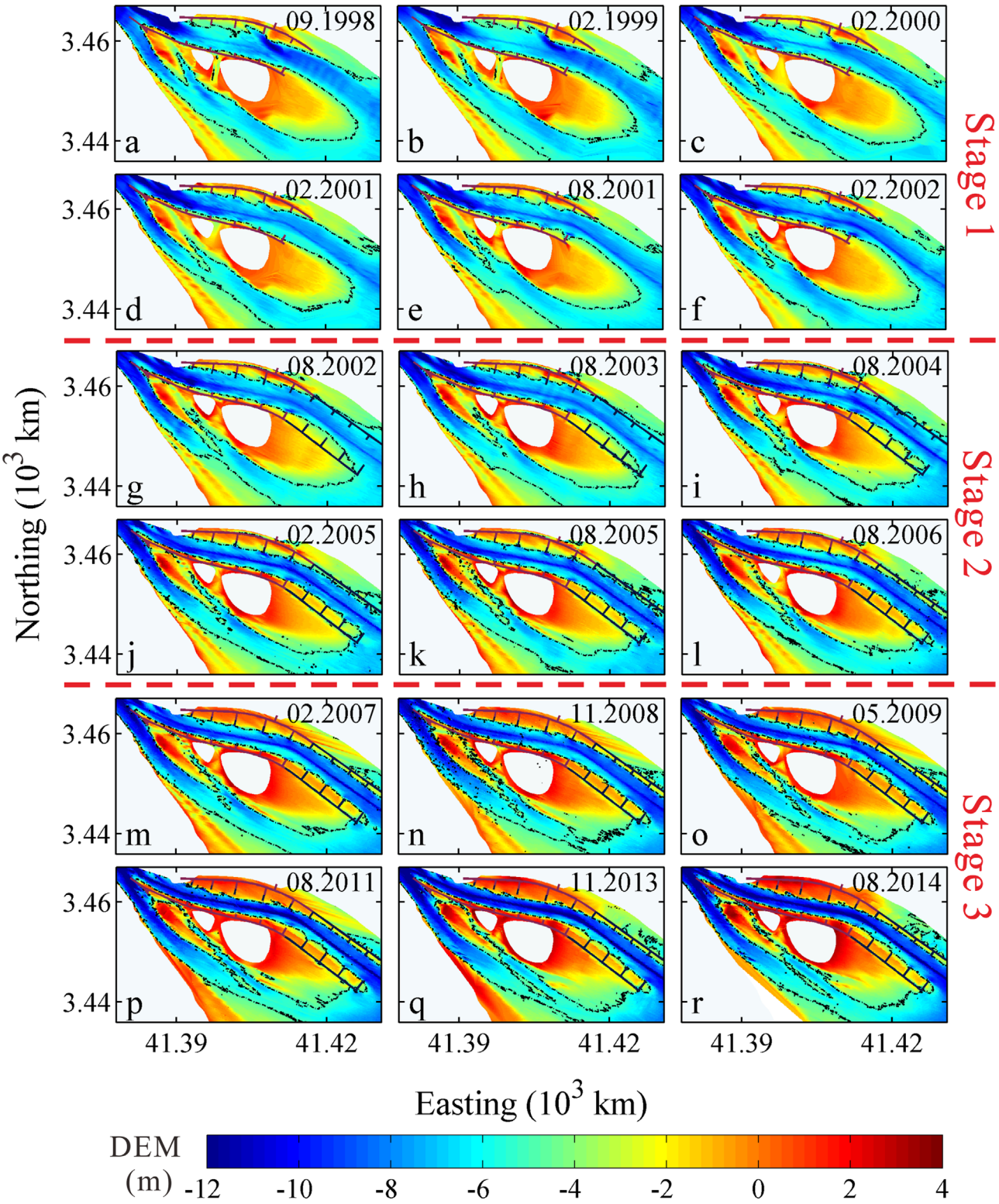

Fig. 4. Representative DEM of JDS in each stage, dark dotted line represents −5 m isobaths of the whole region while purple and dark blue line denotes dike and groins constructed in the 1st and 2nd phase of DWP, respectively. Panels (a-f) indicate Stage 1; (g-l) indicate Stage 2; and (m-r) indicate Stage 3. (For interpretation of the references to color in this figure legend, the reader is referred to the web version of this article.)

Lower Shoal are the most characteristic, where higher and lower flats experience opposite changes, with higher flats retreating a large distance while the lower ones advancing a lot, especially in 11.2008 and 11.2003. Northward expanding is significant again, mainly in 05.2009. Jiangya shoal-creek system evolves as before, with significant stretching in 02.2007 and 08.2011. Jiangya creek is nearly connected to the South Passage at both ends by −5 m isobaths and grows narrower at the same time (Fig. 5e and f). Erosion of south Middle Shoal is severe with continuous stretching of JYS.

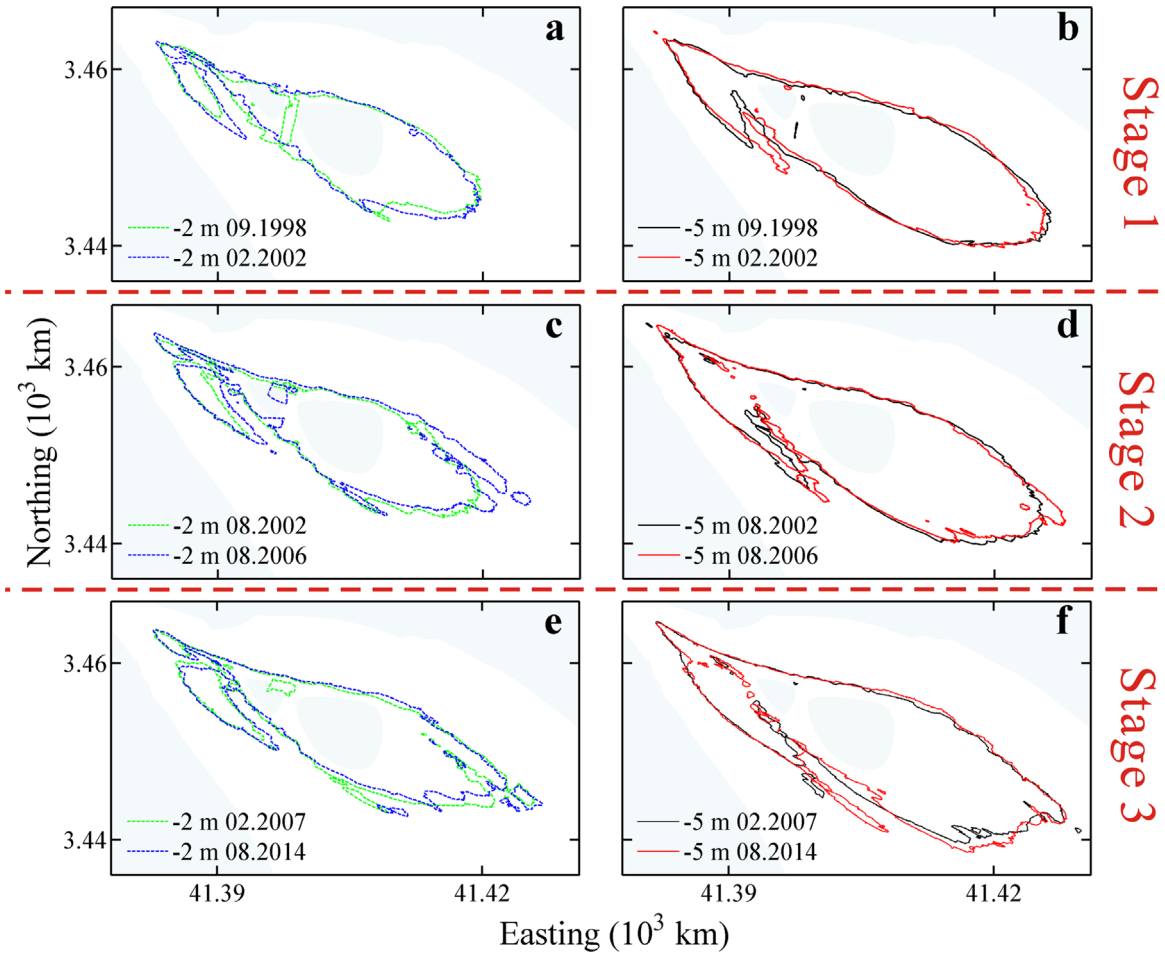

Fig. 5. Inner-stage evolution for isobaths of JDS, with (a, b) isobaths above −2 m and −5 m in Stage 1; (c, d) and (e, f) for those in Stage 2 and 3, respectively.

3.3. Eigenanalysis of bathymetric changes of JDS

Evolution of JDS with DWP proceeding is complicated with interlaced temporal and spatial information (Fig. 4). 2 modes explaining 94% variances of the time-and-space correlated bathymetric changes are decomposed (Fig. 7), which is adequate to represent evolution of JDS.

The first mode undertakes the primary change mode of JDS with a contribution of 88% to the deviations. The first eigenvector reflects basic morphology of JDS after dike construction, within which the readjusted Jiangya shoal-creek system and characteristic shape along the south dike are shown (Fig. 7b). The first eigenweighing presents ladder-like increasing mode, which is statistically significant correlated to cumulative deposition volume of JDS and surrounding channels ($n=35$, $p<0.001$; Fig. 7a). Thus, the first mode represents integral evolution mode of JDS and surrounding channels.

The second mode explains 6% of variances. Eigenvector of this mode is prominent by high absolute values around JYS, along the south dike and south Middle and Lower Shoal, which correspond well with zones experiencing significant bathymetric changes (Figs. 4 and 7d). Considering the continuous decreasing trend of eigenweighing, this mode explains the major regional deposition/erosion of JDS, with significant siltation at north of the south dike and eastern JYS, but erosion at other areas (Fig. 7c). Besides, those regional deposition/erosion will affect area evolution of JDS. Locations of these high absolute eigenvector values, the sharp decreasing eigenweighing during the second stage and the relative stable eigenweighing in Stage 1 reflect changes of area above −2 m ($n=35$, $r=-0.88$, $p<0.01$). A pitch point occurs in the second eigenweighing around 08.2006, which is the end of Stage 2, indicating differences between the first 2 stages and Stage 1. This phenomenon can be explained by the construction of artificial facilities in the first 2 stages.

4. Discussion

4.1. Evolution modes of JDS

During the first 40 years after formation, JDS is eager to grow and experiences a high pace expanding, with area above −5 m increasing nearly once, from 208 km^2 to 387 km^2 (Wei et al., 2015). However, recent expanding of JDS is slight, with area above −5 m increasing by just 9.6% during 1998–2014 (Fig. 2; Table 2). Thus JDS has transformed from high expanding mode to slow expanding mode, which is dominated by significant regional deposition/erosion (Figs. 2–7).

In general, vertical accretion of JDS is more significant than horizontal, considering more dramatic increase of area above 0 m (Fig. 2). Morphology of JDS presents stage changes despite continuous stretching of JYS and northward expanding of JDS (Fig. 8a and d). In Stage 1, bathymetric changes concentrates on landward half of JDS except reshaping of −2 m isobaths on Lower Shoal, including northward expanding with wavy morphology formation, stretching of JYS and migration of Jiangya Creek. Area above all depths increases a lot except that above 0 m due to slight siltation on high flat (Fig. 8a and b). During Stage 2, with continuous

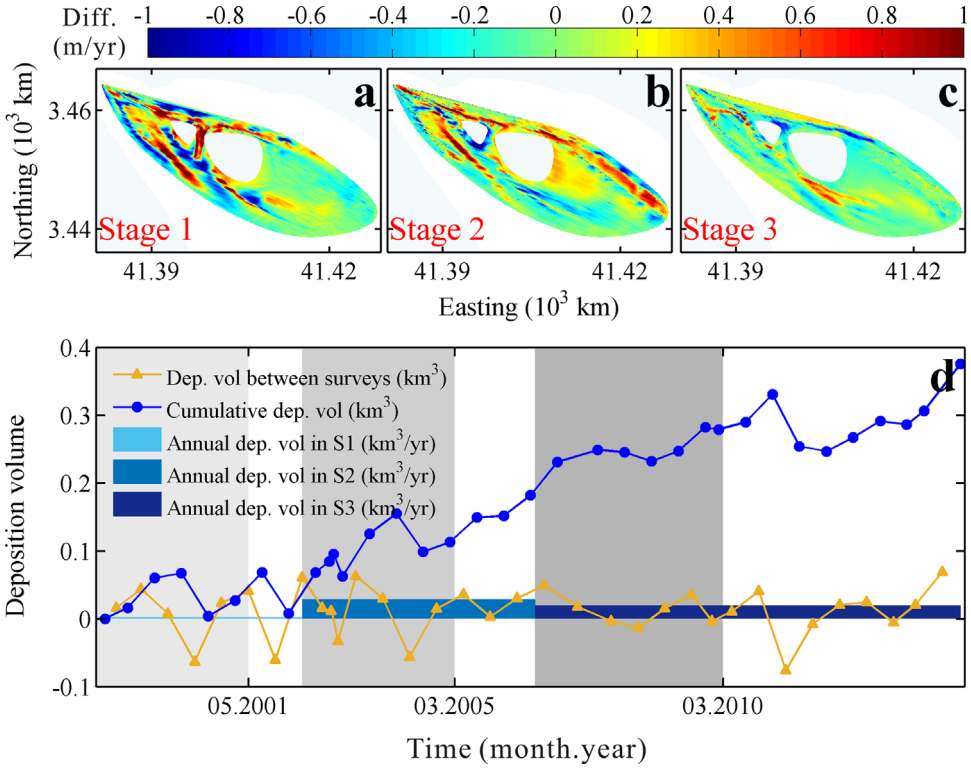

Fig. 6. Inner-stage bathymetric changes of JDS and corresponding deposition volume changes. Panels (a, b and c) depict inner-stage bathymetric changes of JDS within study area in Fig. 1c. Panel (d) represents secular changes of JDS deposition volume (orange solid line marked by triangle), cumulative deposition volume (blue solid line marked by circles) and annual deposition volume within different stages (blue bar). The same as Fig. 2, engineering phases are depicted by grey areas. (For interpretation of the references to color in this figure legend, the reader is referred to the web version of this article.)

evolution of Jiangya shoal-creek system, wavy morphology spreads downstream to cover all groin zone. An erosion band appears south of dike on Lower Shoal and significant siltation occurs north of dike, with area above 0 m and −2 m increasing significantly. Both ends of JDS expand a lot due to siltation along dike (Fig. 8b and c). Stage 3 is an adjustment period for JDS, with erosion band recovery. It is characterized by polarization evolution mode for flats around −2 m and −5 m, despite former evolution of JYS continues (Fig. 8c and d). In this stage, area above 0 m increases a lot due to continuous siltation on flats above 0 m, area above −2 m decreases greatly and area above −5 m increases slightly (Fig. 2).

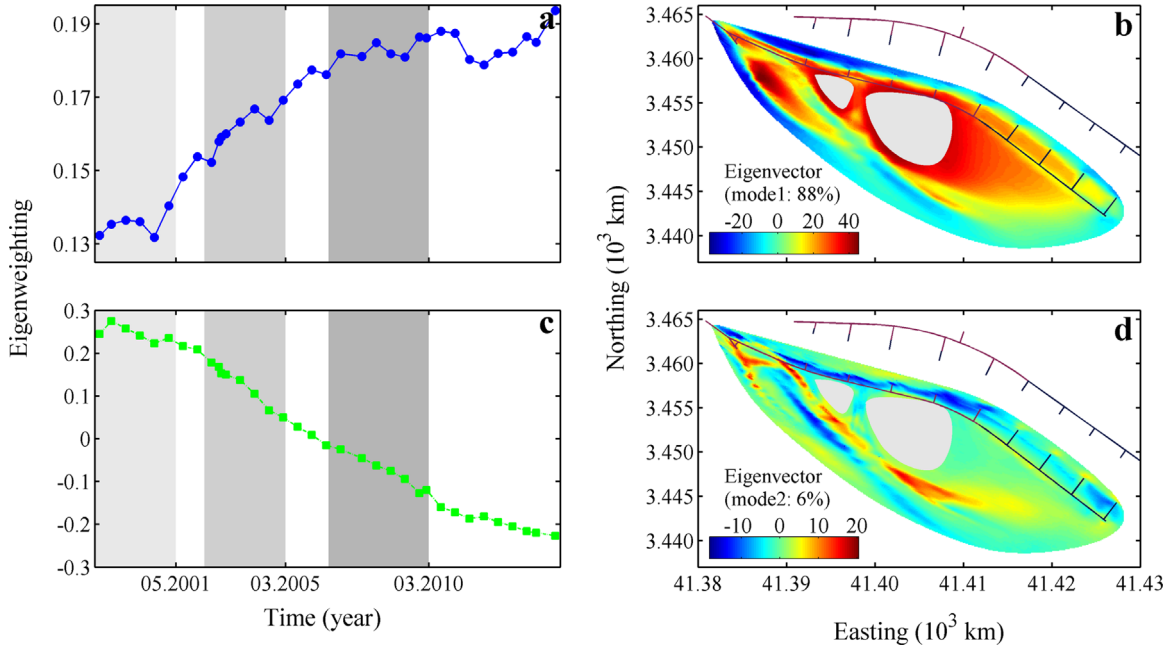

Fig. 7. Results of EOF analysis showing eigenweighings of the first 2 modes (a, c) and contoured eigenvectors of the first 2 modes (b, d). Engineering phases are depicted by grey areas following Fig. 2. Contribution rates of the first 2 modes are labeled in panel b and d.

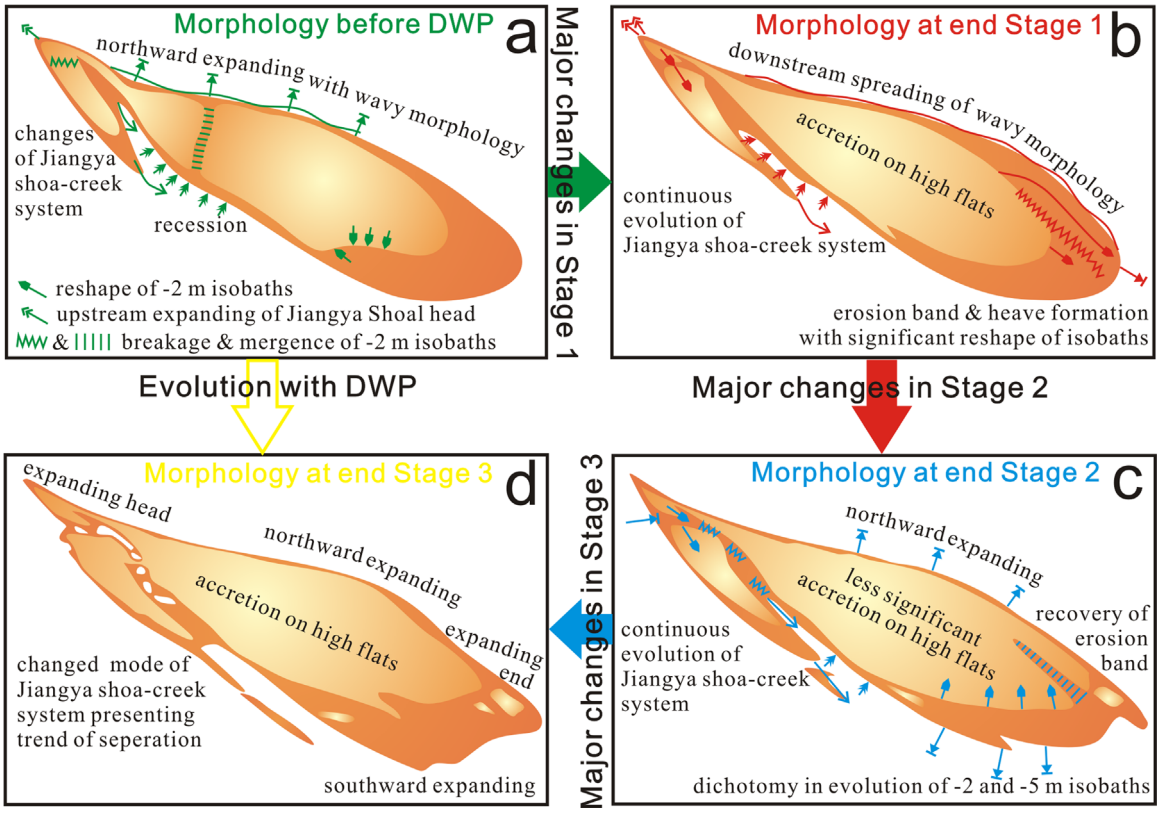

Fig. 8. Graphical representation for evolution of JDS, with (a) morphology of JDS before DWP and corresponding bathymetric changes during Stage 1; (b) morphology at end Stage 1 and changes during Stage 2; (c) morphology at end Stage 2 and changes during stage 3; and (d) final state of JDS after years of adjustment since accomplishment of DWP and major changes relative to state before DWP. Times when corresponding significant bathymetric changes occurs are labeled.

4.2. *Impacts of riverine loads variations*

It's recognized that estuarine shoal growth used to be governed by fluvial load, which, however, has been destroyed by great events, such as regional shoal separation/mergence and giant estuarine engineering (Yang et al., 2003, 2011; Gao et al., 2011; Dai et al., 2014). Recent JDS experiences great changes both in riverine load due to TGD operation and hydrodynamic environment due to DWP proceeding, together with continuous natural processes, whose evolution is more elusory and all factors should be synthesized.

Sediment input to Yangtze estuary has decreased dramatically with peak values decreasing by 70% since TGD operation (Fig. 9c). However, area of JDS increases gradually and presents no notable correlations with inter-survey sediment load and there are periods when area of JDS increases more quickly after TGD operation, such as in Stage 3, which indicates little effect of TGD on integral growth of JDS through altering distal sediment input. This coincides with the findings of Jiang et al. (2012), and similar phenomena have been observed in South Passage and submarine delta

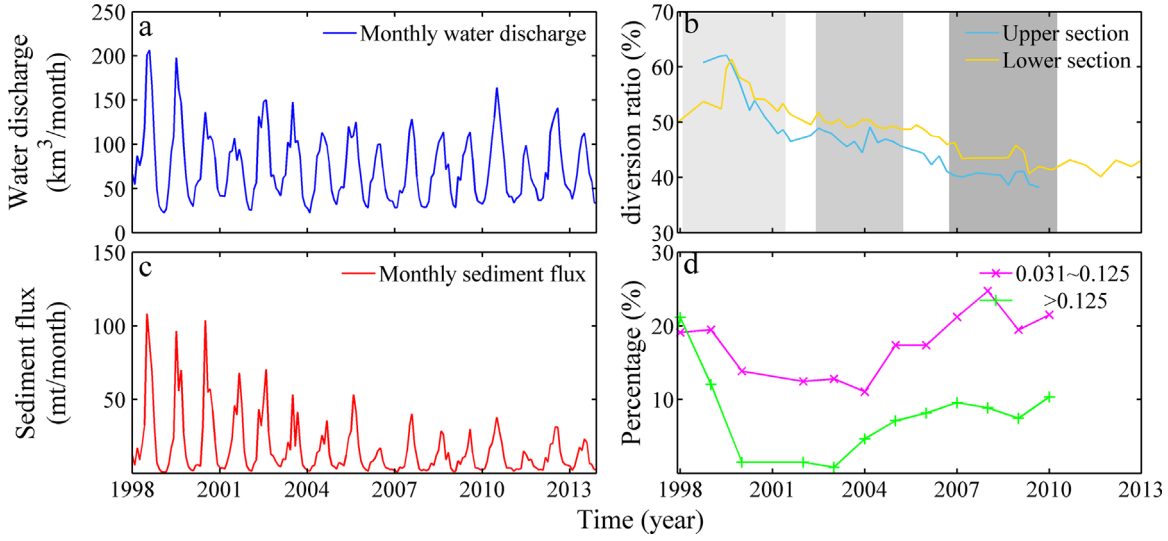

Fig. 9. Changes in riverine loads from Yangtze River, (a, c) monthly water discharge and sediment flux from Yangtze River at Datong station; (b) changes in the ebb flow diversion ratio of North passage through the upper and lower given section; and (d) changes in fraction content of suspended sediment from Yangtze River at Datong Station.

of the Yangtze Estuary, neither of which were infected by TGD (Dai et al., 2014, 2015). Relatively, accretion of JDS may benefit from proximal sediment sources considering slight changes in surrounding suspended sediment concentration (Gao et al., 2008; Liu et al., 2010; Dai et al., 2012). Similar to sediment flux, relative stable water discharge during 1998–2013 plays slight role in JDS growth (Fig. 9c). Coarsening of suspended sediment from Yangtze River shown by Fig. 9c, which results from channel erosion due to sediment entrapped in TGD (Dai and Liu, 2013), may be beneficial to growth of JDS considering the dominance of sand or silt in surface sediment grain fraction as sampled in 2007 (Yan et al., 2011; Luo et al., 2012). Thus changes of riverine load due to TGD has slight impact on gradually expanding of JDS.

Fluctuations in area changes could also be found in other shoals of Yangtze Estuary, like Chongming Shoal and Nanhui Shoal (Yang et al., 2001). Relative to secular tendency, annual fluctuation is prominent in water discharge series, which is dominated by East Asian Summer Monsoon (Wei et al., 2014). Fluctuation of 48 months is also obvious due to ENSO (Gao et al., 2015). Considering relative stable ocean dynamics in Yangtze Estuary in terms of relatively stable tidal range (Jiang et al., 2012), fluctuations in water discharge is the reflection of fluctuations in magnitude of river-sea interaction and seems to control intrinsic annual-quadrennial fluctuations in area changes of JDS, which is documented by lag correlation between them. Specifically, annual-quadrennial fluctuations in area changes have lag time of 3 and 11 months after corresponding fluctuations in water discharge, respectively (Fig. 10). As for area above −2 m and 0 m, they are relatively less affected by the seasonal discharge and tidal current due to vegetation and constructions. Accordingly, periodic fluctuations in area above −2 m and 0 m are insignificant.

4.3. Impacts of Deep Waterway Project

DWP seems to play dominated role in gradual expanding of JDS, which expands northward in the north edge, retreats northward in south edge of the Upper and Middle Shoal, and expands southward in south edge of the Lower Shoal, transforming from original shuttle shape to malformed shape (Fig. 4). DWP operation significantly alters the regional hydrodynamics, which further impacts JDS evolution in a variety of means. Firstly, resistance produced by groins decreases regional flow velocity (Hu and Ding, 2009), inducing significant siltation in groin region and promoting continuous northward expanding of JDS (Figs. 4–6). Secondly, since the DWP constructions are 0.33 m above the mean sea level, flood flow in Jiangya Creek could not enter into the North Passage without restriction, but gets bifurcated approaching the south dike (Hu et al., 2009). Bifurcated branch of flood flow along south dike induces erosion of JYS head. Accordingly, backflow along the JYS facilitates stretching of JYS. Thirdly, the south dike could converge flood flow and enhances flood flow velocity on Lower Shoal, shown by intensified northwestern residual transport south Lower Shoal (Wu et al., 2010), which helps to account for accelerating accretion on flats above 0 m by providing more suspended sediment and subsequent polarization evolution mode for flats around −2 m and −5 m on Lower Shoal. Fourthly, DWP, especially the diverting work in the 1st phase, changes ebb flow ratio between the North Passage and the South Passage significantly (Hu and Ding, 2009). With dramatic increase in ebb flow diversion ratio of the South Passage (Fig. 9b), ebb flow in upper South Passage is strengthened shown by higher flow dominance value (Dai et al., 2015), which pushes JYS tail migrating downward, results in thinner of Jiangya Creek and induces erosion of south Middle Shoal. Variations in area changes of JDS above different depths and in different stages are due to constructions of different engineering phases.

4.4. Impacts of green engineering

Vegetation plant in green engineering could accelerate shoal accretion through attenuating hydrodynamics and trapping sediments (Wang et al., 2013), which could also account for area increase of JDS above 0 m. However, green engineering's impact on area changes above −2 m and −5 m is slight because vegetation

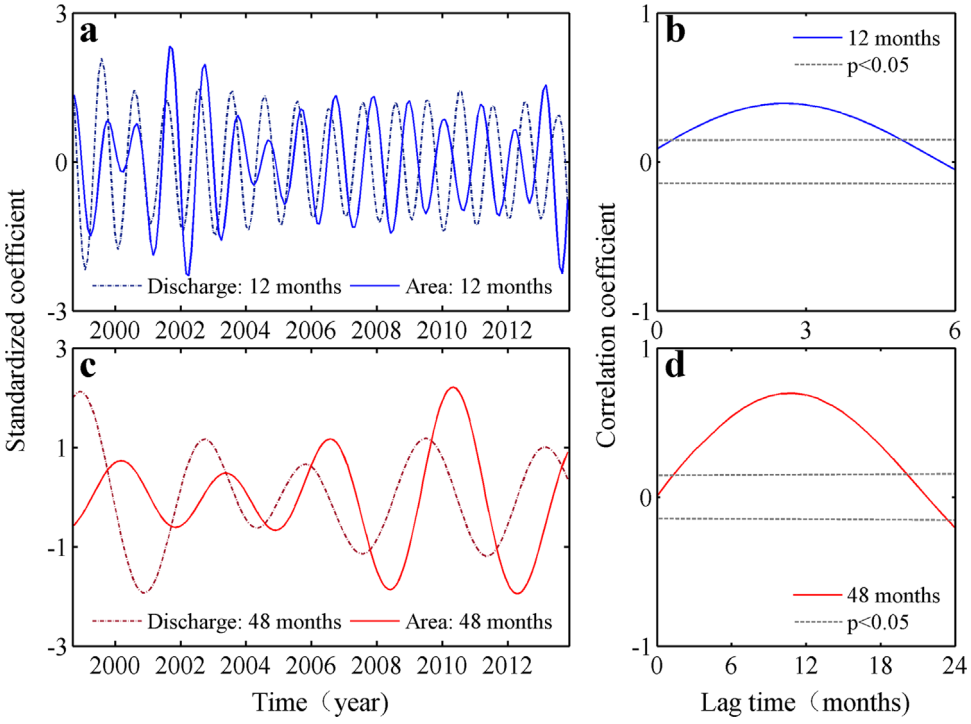

Fig. 10. Relations between water discharge and area change of JDS above −5 m: (a, c) extracted periodic components of 1 and 3–4 years from wavelet contoured coefficient, similar to those in Fig. 3b; and (b, d) lag correlation between periodic components of water discharge and area change of JDS above −5 m.

mainly locates in supratidal zone and upper intertidal zone. This could be documented by variations in area above 0 m and −2 m (Fig. 2). In Stage 3, area above 0 m continues increasing while area above −2 m decreases slightly, indicating that DWP induced intensified flood flow in Lower Shoal plays more significant role in area change above −2 m.

Moreover, the seasonal wave dynamics in Yangtze Estuary is characterized by southeastward wave in summer and northwestward wave in winner (Shi, 2001), which may induce seasonal conversion between siltation and erosion. However, the southeastward wave is blocked by the south dike of DWP, and finally reaches JDS in terms of refraction and diffraction with significantly reduced wave energy. Therefore, JDS's morphodynamic evolution is dominated by northwestward wave with minor impacts from southeastward wave action (Fig. 4).

5. Conclusions

Morphodynamic evolution of estuarine distributary bar is a well demonstration of artificial interference on estuary and is prominent in evolution of lateral passages. Based on unique high-resolution seasonal-surveyed digital topographic data, recent evolution of JDS, the largest uninhabited island in the Yangtze Estuary, is explored. Meaningful conclusions are shown as follows:

1) JDS has turned from a rapid growing status to a slight increasing status with area above −5 m increasing just 9% during 1998–2014. Meanwhile, JDS is more inclined to grow higher than larger, with relative high increasing rate of 4.57 km^2/yr for area above 0 m. Periodic signals of 12 and 48 months are involved in area changes of JDS.
2) Despite continuous stretching of JYS, morphodynamic evolution of JDS presents stage modes as follows: Significant siltation occurs north of upstream JDS with less siltation on high flats during1998–2002; During 2002–2006, JDS evolution is characterized by erosion band appearing just south of dike on Lower Shoal and siltation on north edge of seaward JDS, meanwhile high flats accrete significantly; After 2007, former erosion band recovers and south Lower Shoal presents polarization evolution mode, with flats around −2 m retreat but those around −5 m expanding southward.
3) DWP controls expanding trend, regional deposition/erosion and sandbar migration of JDS through altering local flow magnitude and changing flow paths. Green engineering could affect area increase above 0 m, but play slight role in area changes above −2 m and −5 m. Streamflow controls periodic evolution of JDS, while distal sediment input from Yangtze River has little effect on recent sedimentation of JDS.

Acknowledgements

This study was supported by the Funds from the National Natural Science Foundation of China (NSFC) (Grant number: 41476076 and 41376097). We gratefully acknowledge Prof. Zhongyuan Chen for his valuable suggestion in preliminary version.

References

Ashley, G.M., 1990. Classification of large scale subaqueous bedforms: a new look at an old problem. J. Sediment. Petrol. 60, 160–172.
Bale, A.J., Uncles, R.J., Villena Lincoln, A., Widdows, J., 2007. An assessment of the potential impact of dredging activity on the Tamar estuary over the last century: bathymetric and hydrodynamic changes. Hydrobiologia 588, 83–95.
Bartholdy, J., Flemming, B.W., Bartholoma, A., Ernstsen, V.B., 2005. Flow and grain size control of depth-independent simple subaqueous dunes. J. Geophys. Res. 110, F04S16.
Benedet, L., List, J.H., 2008. Evaluation of the physical process controlling beach changes adjacent to nearshore dredge pits. Coast. Eng. 55, 1224–1236.
Blott, S.J., Pye, K., van der Wal, D., Neal, A., 2006. Long-term morphological change and its causes in the Mersey Estuary, NW England. Geomorphology 81 (1–2), 185–206.
Blum, M.D., Roberts, H.H., 2009. Drowning of the Mississippi Delta due to insufficient sediment supply and global sea-level rise. Nat. Geosci. 2, 488–491.
Carling, P.A., Golz, E., Orr, H.G., Radecki-Pawlik, A., 2000. The morphodynamics of fluvial sand dunes in the River Rhine, near Mainz, Germany. Part I. Sedimentology and morphology. Sedimentology 47, 227–252.
Chaumillon, E., Bertin, X., Falchetto, H., Allard, J., Weber, N., Walker, P., Pouvreau, N., Woppelmann, G., 2008. Multi time-scale evolution of a wide estuary linear sandbank, the Longe de Boyard, on the French Atlantic coast. Mar. Geol. 251 (3–4), 209–223.
Chen, J.Y., Li, D.J., Chen, B.L., Hu, F.X., Zhu, H.F., Liu, C.Z., 1999. The processes of dynamic sedimentation in the Changjiang Estuary. J. Sea Res. 41, 129–140.
Corbetta, D.R., McKeeb, B., Allisonb, M., 2006. Nature of decadal-scale sediment accumulation on the western shelf of the Mississippi River delta. Cont. Shelf Res. 26 (17–18), 2125–2140.
Cuadrado, D.G., Gómez, E.A., Ginsberg, S.S., 2003. Large transverse bedforms in a mesotidal estuary. J. Argent. Assoc. Sedimentol. 10, 163–172.
Dai, Z.J., Liu, J.T., Lei, Y.P., Zhang, X.L., 2010. Patterns of sediment transport pathways on a headland bay beach-Nanwan beach, South China: a case study. J. Coast. Res. 26 (6), 1096–1103.
Dai, Z.J., Chu, A., Li, W.H., Wu, H.L., 2012. Has suspended sediment concentration near the mouth bar of the Yangtze (Changjiang) Estuary been declining in recent years? J. Coast. Res. 29 (4), 809–818.
Dai, Z., Liu, J.T., 2013. Impacts of large dams on downsteram fluvial sedimentation: an example of the three gorges dam (TGD) on the Changjiang (Yangtze River). J. Hydrol. 48, 10–18.
Dai, Z., Liu, J.T., Wei, W., Chen, J., 2014. Detection of the Three Gorges Dam influence on the Changjiang (Yangtze River) submerged delta. Sci. Rep. 4, 6600. http://dx.doi.org/10.1038/srep06600.
Dai, Z.J., Liu, J.T., Wen, W., 2015. Morphological evolution of the South Passage in the Changjiang (Yangtze River) estuary, China. Quat. Int. 187, 101–107.
Fanos, A.M., 1995. The impact of human activities on the erosion and accretion of the Nile delta coast. J. Coast. Res. 11, 821–833.
Flemming, B.W., 1978. Underwater sand dunes along the southeast African continental margin-observations and implications. Mar. Geol. 26, 177–198.
Francken, F., Wartel, S., Parker, R., Taverniers, E., 2004. Factors influencing subaqueous dunes in the Scheldt Estuary. Geo-Mar. Lett. 24, 14–24.
Gao, A., Yang, S.L., Li, G., Li, P., Chen, S.L., 2010. Long-term morphological evolution of a tidal island as affected by natural factors and human activities, the Yangtze Estuary. J. Coast. Res. 261, 123–131.
Gao, J.J., Dai, Z.J., Mei, X.F., et al., 2015. Interference of natural and anthropogenic forcings on variations in continental freshwater discharge from the Red River (Vietnam) to sea. Quat. Int. http://dx.doi.org/10.1016/j.quaint.2015.01.007.
Gao, S., Wang, Y.P., 2008. Changes in material fluxes from the Changjiang River and their implications on the adjoining continental shelf ecosystem. Cont. Shelf Res. 28 (12), 1490–1500.
Gao, S., Wang, Y.P., Gao, J.H., 2011. Sediment retention at the Changjiang sub-aqueous delta over a 57 year period, in response to catchment changes. Cont. Shelf Res. 95 (1), 29–38.
Harbor, D.J., 1998. Dynamics of bedforms in the lower Mississippi River. J. Sediment. Res. 68, 750–762.
Harrisa, P.T., Hughesb, M.G., Bakerb, E.K., et al., 2004. Sediment transport in distributary channels and its export to the pro-deltaic environment in a tidally dominated delta: Fly River, Papua New Guinea. Cont. Shelf Res. 24 (19), 2431–2454.
Hu, K., Ding, P., 2009. The effect of deep waterway constructions on hydrodynamics and salinities in Yangtze Estuary, China. J. Coast. Res. SI56, 961–965.
Hu, K., Ding, P.X., Wang, Z.B., Yang, S.L., 2009. A 2D/3D hydrodynamic and sediment transport model for the Yangtze Estuary, China. J. Mar. Syst. 77 (12), 114–136.
Jaffe, B.E., Smith, B.E., Smith, R.E., Foxgrover, A.C., 2007. Athropogenic influence on sedimentation and intertidal mudflat change in San Pablo Bay, California: 1856–1983. Estuar. Coast. Shelf Sci. 73, 175–187.
Jia, L.W., Pan, S.Q., Wu, C.Y., 2013. Effects of the anthropogenic activities on the morphological evolution of the Modaomen Estuary, Pearl River Delta, China. China Ocean Eng. 27 (6), 795–808.
Jiang, C.J., Li, J.F., de Swart, H.E., 2012. Effects of navigational works on morphological changes in the bar area of the Yangtze Estuary. Geomorphology 139–140, 205–219.
Kim, T.I., Choi, B.H., Lee, S.W., 2006. Hydrodynamics and sedimentation induced by large-scale coastal developments in the Keum River Estuary, Korea. Estuar. Coast. Shelf Sci., 515–528.
Kostaschuk, R.A., Church, M.A., Luternauer, J.L., 1989. Bedforms, bed material, and bedload transport in a salt-wedge estuary: Fraser River, British Columbia. Canadian. Can. J. Earth Sci. 26, 1440–1452.
Lafite, R., Romaña, L.A., 2001. A man-altered macrotidal estuary: the Seine estuary (France): introduction to the special issue. Estuaries 24 (68), 939.
Lee, H.J., Ryu, S.O., 2008. Changes in topography and surface sediments by the Saemangeum dyke in an estuarine complex, west coast of Korea. Cont. Shelf Res. 28 (9), 1177–1189.
Liu, G., Zhu, J., Wang, Y., Wu, H., Wu, J., 2010. Tripod measured residual currents and

sediment flux: Impacts on the silting of the Deepwater Navigation Channel in the Changjiang Estuary. Estuar. Coast. Shelf Sci. 93 (3), 192–201.
Luo, X.X., Yang, S.L., Zhang, J., 2012. The impact of the Three Gorges Dam on the downstream distribution and texture of sediments along the middle and lower Yangtze River (Changjiang) and its estuary, and subsequent sediment dispersal in the East China Sea. Geomorphology 179, 126–140.
McLoughlin, L.C., 2000. Shaping Sydney Harbour: Sedimentation, dredging and reclamation 1788–1990s. Aust. Geogr. 31 (2), 183–208.
Milliman, J.D., Qin, Y.-S., Ren, M.-E., Saito, Y., 1987. Man's influence on the erosion and transport of sediment by Asian rivers: the Yellow River (Huanghe) example. J. Geol. 95, 751–762.
Nagarajana, R., Jonathanb, M.P., Royc, P.D., et al., 2015. Decadal evolution of a spit in the Baram river mouth in eastern Malaysia. Cont. Shelf Res. 105, 18–25.
Rubin, D.M., McCulloch, D.S., 1980. Single and superimposed bedforms: a synthesis of San Francisco Bay and flume observations. Sediment. Geol. 26, 207–231.
Ramsar, C.S., 2007. National wetland policies: developing and implementing national wetland policies. In: Ramsar Handbooks for the Wise Use of Wetlands, third ed., Vol. 2. Ramsar Convention Secretariat, Gland, Switzerland.
Raston, D.K., Geyer, W.R., Traykovski, P.A., et al., 2013. Effects of estuarine and fluvial processes on sediment transport over deltaic tidal flats. Cont. Shelf Res. 60 (15), S40-457.
Shi, Z., 2001. Studies on hydrodynamic processes (1979–1999) in the Changjiang RIVER Estuary. Mar. Sci. 25 (6), 54 57.
Syvitski, J.P.M., Vörösmarty, C.J., Kettner, A.J., Green, P., 2005. Impact of Humans on the Flux of Terrestrial Sediment to the Global coastal ocean. Science 308, 376–380.
Syvitski, J.P.M., Saito, Y., 2007. Morphodynamics of deltas under the influence of humans. Glob. Planet. Change 57 (3–4), 261–282.
Torrence, C., Compo, G.P., 1998. A practical guide to wavelet analysis. Bull. Am. Meteorol. Soc. 79 (1), 61–78.
Van der Wal, D., Pye, K., Neal, A., 2002. Long-term morphological change in the Ribble estuary, Northwest England. Mar. Geol. 189, 249–266.
Van der Wal, D., Pye, K., 2003. The use of historical bathymetric charts in a GIS to assess morphological change in estuaries. Geogr. J. 169 (1), 21–31.
Wang, Q., Jorgensen, S.E., Lu, J.J., Nielsen, S.N., Zhang, J.R., 2013. A model of vegetation dynamics of Spartina alterniflora and Phragmites australis in an expanding estuarine wetland: biological interactions and sedimentary effects. Ecol. Model. 250, 195–204.
Wang, Y.H., Dong, P., Oguchi, T., 2013. Long-term (1842–2006) morphological change and equilibrium state of the Changjiang (Yangtze) Estuary, China. Cont. Shelf Res. 56, 71–81.
Wei, W., Chang, Y.P., Dai, Z.J., 2014. Streamflow changes of the Changjiang (Yangtze) River in the recent 60 years: impacts of the East Asian summer monsoon, ENSO, and human activities. Quat. Int. 336, 98–107.
Wei, W., Tang, Z.H., Dai, Z.J., Lin, Y.F., Ge, Z.P., Gao, J.J., 2015. Variations in tidal flats of the Changjiang (Yangtze) Estuary during 1950s–2010s: future crisis and policy implication. Ocean Coast. Manag. 108, 89–96.
Wu, H., Zhu, J., Choi, B., 2010. Links between salt water intrusion and subtidal circulation in the Changjiang Estuary: a model-guided study. Cont. Shelf Res. 30, 1891–1905.
Xie, X.P., Wang, Z.Y., Asce, M., et al., 2009. Formation and evolution of the Jiuduansha Shoal over the past 50 years. J. Hydraul. Eng. 135 (9), 741–754.
Xu, J.X., 2008. Response of land accretion of the Yellow River delta to global climate change and human activity. Quat. Int. 186 (1), 4–11.
Yan, H., Dai, Z.J., LI, J.F., et al., 2011. Distributions of sediments of the tidal flats in response to dynamic actions, Yangtze (Changjiang) Estuary. J. Geogr. Sci. 21 (4), 719–732.
Yang, S.L., Zhao, Q.Y., Chen, S.L., 2001. Seasonal changes in coastal dynamics and morphological behavior of the central and southern Changjiang River delta. Sci. China (Ser. B) 44, 72–79.
Yang, S.L., Belkin, I.M., Belkina, A.I., Zhao, Q.Y., Zhu, J.R., Ding, P.X., 2003. Delta response to decline in sediment supply from the Yangtze River: evidence of the recent four decades and expectations for the next half-century. Estuar. Coast. Shelf Sci. 57, 689–699.
Yang, S.L., Milliman, J.D., Li, P., Xu, K., 2011. 50,000 dams later: erosion of the Yangtze River and its delta. Glob. Planet. Change 75, 14–20.
Yoo, C., Kim, S., 2004. EOF analysis of surface soil moisture field variability. Adv. Water Resour. 27, 831–842.
Yun, C.X., 2010. Illustrated Handbook on Evolution of Yangtze Estuary. China Ocean Press, Beijing.
Zheng, J.H., Peng, Y.X., Zhang, C., 2013. Recent evolution of Jiuduansha Shoal in Yangtze Estuary and its corresponding to engineering projects. J. Coast. Res. 65, 1259–1264.